



# Manipulating the chaos bandwidth of a semiconductor laser subjected to phase-conjugate feedback

Guillaume Bouchez, Tushar Malica, Delphine Wolfersberger, Marc Sciamanna

## ► To cite this version:

Guillaume Bouchez, Tushar Malica, Delphine Wolfersberger, Marc Sciamanna. Manipulating the chaos bandwidth of a semiconductor laser subjected to phase-conjugate feedback. Semiconductor Lasers and Laser Dynamics IX, Apr 2020, Online Only, France. pp.113560Y, 10.1117/12.2559627 . hal-03565029

**HAL Id: hal-03565029**

**<https://hal.science/hal-03565029>**

Submitted on 10 Feb 2022

**HAL** is a multi-disciplinary open access archive for the deposit and dissemination of scientific research documents, whether they are published or not. The documents may come from teaching and research institutions in France or abroad, or from public or private research centers.

L'archive ouverte pluridisciplinaire **HAL**, est destinée au dépôt et à la diffusion de documents scientifiques de niveau recherche, publiés ou non, émanant des établissements d'enseignement et de recherche français ou étrangers, des laboratoires publics ou privés.

# Manipulating the chaos bandwidth of a semiconductor laser subjected to phase-conjugate feedback

Guillaume Bouchez<sup>a,b</sup>, Tushar Malica<sup>a,b</sup>, Delphine Wolfersberger<sup>a,b</sup>, and Marc Sciamanna<sup>a,b</sup>

<sup>a</sup>Chaire Photonique, LMOPS, CentraleSupélec, 2 Rue Edouard Belin, 57070 Metz, France

<sup>b</sup>Université de Lorraine, LMOPS, 2 Rue Edouard Belin, 57070 Metz, France

## ABSTRACT

In this manuscript, we study the influence of various parameters on the dynamics of a semiconductor laser with phase-conjugate feedback. We report the chaos bandwidth of its chaotic states, and simultaneously the frequency of its self-pulsing modes. We demonstrate that both indicators are unaffected by the delay length at any given feedback strength. A higher pumping current enhances both indicators, as does an increase of the carrier lifetime. We further investigate the influence of the linewidth enhancement factor ( $\alpha$ -factor): restabilization occurs for higher values of feedback strength, thereby enhancing the system's limit of attaining higher values of the chaos bandwidth. The effective bandwidth is observed to follow the general trend of the chaos bandwidth with an exception of transition dynamical solutions. We show that the PCF system is able to generate high-frequency and broadband chaos without any additional active optical element. Because of the high quality of chaos induced by the PCF system, delayed laser systems are strong candidate to generate high-performance chaotic signals.

**Keywords:** Phase-conjugate feedback, Chaotic laser diodes, High-frequency dynamics of laser diodes, Complex dynamics of laser diodes

## 1. INTRODUCTION

A semiconductor laser subjected to optical feedback can easily become unstable.<sup>1,2</sup> In particular, it can exhibit regular self-pulsing dynamics, steady-states and chaos, depending on the feedback strength.<sup>3</sup> To observe a wider range of dynamics, a relatively simple way is to introduce the phase-conjugate feedback. For low feedback strength values, chaos appears from the undamping of the relaxation oscillations,<sup>4-7</sup> as in conventional feedback.<sup>8</sup> However, the phase-conjugate feedback chaotic states are more broadband than the chaos obtained with conventional feedback.<sup>9</sup> If we increase the feedback strength, the chaos bandwidth increases, as the chaos centered around the laser relaxation oscillations bifurcates into unique broadband chaos.<sup>10</sup>

Then, the system locks-on completely new dynamics. The output power oscillates at a frequency equal to a multiple of the inverse of the output roundtrip time and this frequency is often higher than the relaxation oscillation frequency.<sup>6,7</sup> Analogous to the external cavity modes of the conventional feedback, these latter states are named external cavity modes (ECMs).<sup>11</sup> For even higher values of feedback, the laser restabilizes into a steady-state solution, ending the chaotic and self-pulsing states.<sup>5,7,12</sup>

Our focus in this study is the influence of the various parameters of the laser and of the external cavity on the frequencies associated with the laser dynamics.

---

Further author information: (Send correspondence to G.B.)

G.B.: E-mail: guillaume.bouchez@centralesupelec.fr, Telephone: +33 (0)3 87 76 59 01

## 2. EXPERIMENTAL AND THEORETICAL BACKGROUND

### 2.1 Typical experimental setup

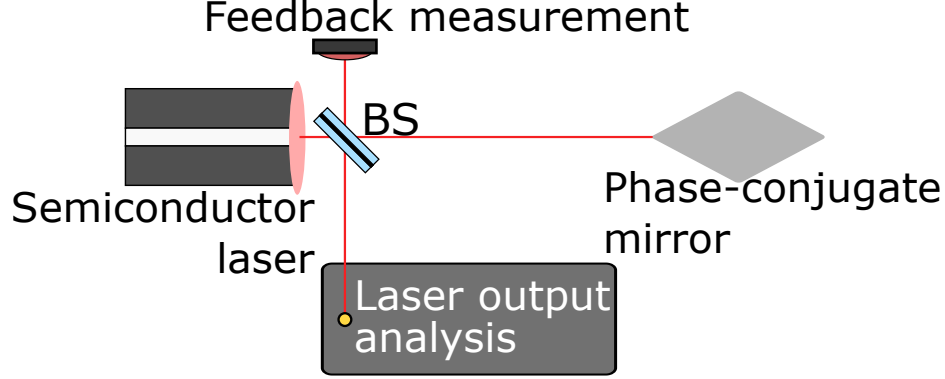


Figure 1. Typical setup of a phase-conjugate feedback experiment.

A typical setup is shown Fig. 1. The output beam from a semiconductor laser is sent to a phase-conjugate mirror. The phase-conjugated beam is reflected back into the laser, while part of this feedback beam is deviated by a beamsplitter (BS) to monitor the feedback strength. The same beamsplitter sends part of the laser output into a analysis system, to enable the study of the laser dynamical states.

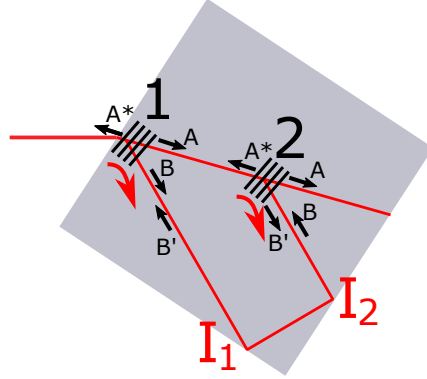


Figure 2. Typical setup of a *cat* self-pumped phase-conjugate mirror. The light enters from the left, part of it is fanned to the bottom and reflected on the edges of the crystal. The phase-conjugate wave is obtained by four-wave mixing in gratings 1 and 2.

Phase-conjugation can be achieved by several means, generally through four-wave mixing in non-linear medias, such as photorefractive crystals.<sup>13</sup> In particular, we have experimentally studied phase-conjugate feedback with rhodium-doped barium titanate crystals, in *cat* self-pumped phase-conjugate mirror configuration (*cat*-SPPCM).<sup>14</sup> In these mirrors, as detailed in Fig. 2, part of the input light is deviated by the photorefractive effect (beam fanning). The deviated light from 1 ( $B$ ) is then reflected on the sides of the crystal (at  $I_1$  and  $I_2$ ). If the geometry enables it, four-wave mixing occurs in 2 between the light that travels in a straight direction  $A$ , the deviated light  $B$  and the light being deviated there  $B'$ . The fourth wave,  $A^*$ , is the backward propagative phase-conjugate of the input beam. Similarly, wave mixing also occurs in grating 1.

### 2.2 Theoretical model

To simulate a laser with phase-conjugate feedback, we are using normalized equations derived from the Lang-Kobayashi equations:<sup>15</sup>

$$\dot{E}(t) = (1 + i\alpha)E(t)N(t) + \gamma F(t) \quad (1)$$

$$T\dot{N}(t) = P - N(t) - (1 + 2N(t))|E(t)|^2 \quad (2)$$

Where,  $E(t)$  is the normalized complex output electric field,  $N(t)$  the normalized carrier density above threshold and  $\gamma F(t)$  the feedback electric field;  $\gamma$  being the feedback ratio.  $\alpha$  is the standard linewidth enhancement factor,  $P$  the pump parameter above threshold and  $T$  the carrier lifetime. All the times are normalized by the photon lifetime.

In an initial approach,  $F(t)$  was equal to the phase-conjugate of the delayed laser output field  $E^*(t-\theta)$ ,  $\theta$  being the roundtrip time delay.<sup>16</sup> This model has been able to reproduce some of the dynamics of the phase-conjugate feedback lasers, such as chaos<sup>17</sup> and ECMs.<sup>11</sup> However, we are not able to obtain steady-state solutions, that have been observed experimentally at high values of feedback. In 1998, a new model was introduced, namely, the filtered phase-conjugate feedback field, to account for the nonlinear interactions in the phase-conjugate feedback.<sup>18</sup> In the case of a *cat*-SPPCM, this filter can be linked to the length of interaction of light between 1 and 2 on Fig. 2. Such a model is able to numerically reproduce the restabilization of the laser via an Hopf bifurcation.<sup>19</sup> Therefore, we introduce the following equations for the feedback output field :

$$\tau_r \dot{F}(t) = E^*(t - \theta) - F(t) \quad (3)$$

$\tau_r$  is named finite penetration depth, and is proportional to the length of the phase-conjugate feedback.<sup>18</sup>

We set the parameters as in table 1, chosen on the basis of a previous study of the position of the external cavity modes.<sup>20</sup> These values have been chosen to simulate a laser with relaxation oscillations of 3.6 GHz, a pumping current equal to 1.6016 times the threshold current, an external cavity single-trip length of 52.5 cm and a cubic phase-conjugate mirror with edges of 5 mm.<sup>7</sup>

Table 1. Typical values of laser and feedback parameters used in this study as default values

parameter	name	value
$\tau_p$	photon lifetime	1.4 ps
$\alpha$	linewidth enhancement factor	2
$P$	pump parameter above threshold	0.6016
$\theta$	normalized delay	2500
$T$	normalized carrier lifetime	1200
$\tau_r$	normalized finite penetration depth	50
$\gamma$	feedback ratio	variable

### 2.3 Studied parameters

Our focus in this manuscript are two key indicators, one for each main dynamical state of the chaos bandwidth. To study the ECMs, we perform an analysis of the frequency of the regular self-pulsing states. The ECMs can be confused with the undamped relaxation oscillations, but these latter solutions can be obtained only at low feedback values.<sup>19</sup> Then, to study the chaotic states, we compute their chaos bandwidth. The chaos bandwidth is an indicator of the performances of a chaotic signal and is defined as the span of frequencies that contains 80% of the total power, starting from the DC frequency. A high chaos bandwidth means that the chaotic signal spans onto high frequencies.<sup>21</sup> We also study the effective chaos bandwidth, defined as the sum of the discrete spectral components that contain 80% of the total power. A high effective chaos bandwidth indicates that the spectrum is broadly distributed on many frequencies.<sup>22</sup>

### 3. NUMERICAL RESULTS

We want to study the influence of the feedback strength  $\gamma$ , of the  $\alpha$ -factor, of the pump  $P$ , of the carrier lifetime  $T$ , of the delay  $\theta$  and of the finite depth penetration  $\theta$ . We use the fourth order Runge-Kutta algorithm with an integration step equal to the carrier lifetime to obtain 4000000 points-long time series, and we perform frequency analysis on time series with regular oscillations and chaos bandwidth analysis on chaotic ones, after the first 50000 points have been removed.

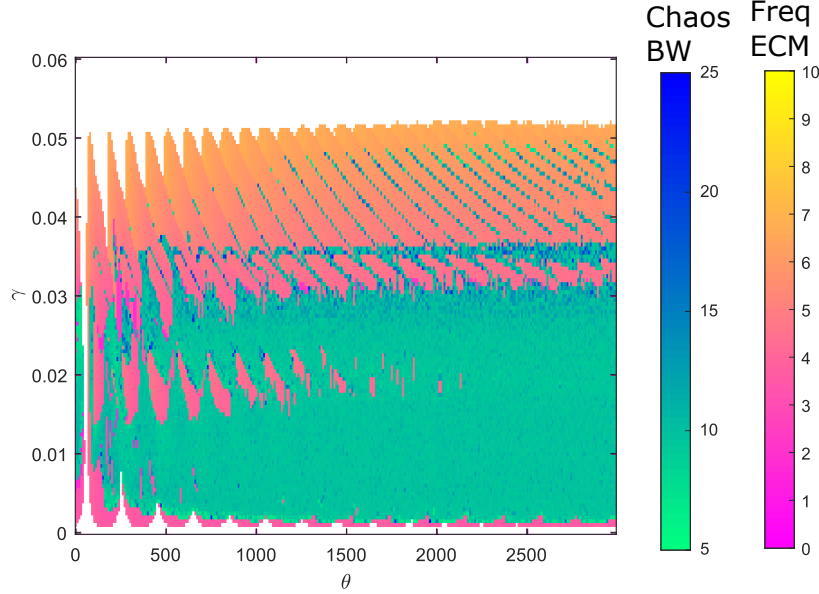


Figure 3. Influence of the delay  $\theta$  (horizontal axis) and of the feedback strength  $\gamma$  (vertical axis) on the frequency of the external cavity modes for the self-pulsing states (pink to yellow color-scales) and on the chaos bandwidth (green to blue color-scales). The steady-states are displayed in white.

We present in Fig. 3 the evolution of the chaos bandwidth and of the frequency of the ECMs versus the feedback strength  $\gamma$  and the normalized delay length  $\theta$ . Simulations of the frequency of the ECMs has already demonstrated it to be globally independent of the delay at a fixed feedback strength, the laser oscillating at the nearest multiple of the external cavity frequency.<sup>23</sup> Our simulation extends this result further to the chaos bandwidth. The chaos bandwidth seems to be independent of the delay at a fixed value of feedback. Between successive external cavity modes, small regions exhibiting chaos bandwidth of up to 25 GHz are observed.

Figure 4 shows the evolution of the chaos bandwidth and of the frequency of the ECMs versus the feedback strength  $\gamma$  and the finite penetration depth in the phase-conjugate mirror,  $\tau_r$ . Previous simulations had shown its influence on the restabilization: increasing  $\tau_r$  decreases the value of the restabilization for the feedback strength.<sup>19</sup> On the other hand, a smaller value of  $\tau_r$  also enables more broadband chaos. Indeed, for  $\tau_r < 10$ , broadband chaos (up to 25 GHz) can be obtained for  $\gamma \approx 0.05$ . However, reducing  $\tau_r$  requires a shorter phase-conjugate mirror, and this may complicate the attainment of high feedback values.

In Fig. 5, we trace the chaos bandwidth and the frequency of ECMs when tuning the  $\alpha$ -factor and the feedback strength  $\gamma$ . For low values of  $\alpha$  ( $\alpha < 0.9$ ), the laser remains stable, which is consistent with the definition of  $\alpha$  as an amplitude-phase coupling responsible for the destabilization of lasers. At a given value of  $\gamma$ , the chaos bandwidth seems to be rather independent from  $\alpha$ . However, decreasing  $\alpha$  forces the transition to ECMs and the restabilization to occur at lower values of  $\gamma$ , and hence the region of high values of chaos bandwidth at high values of  $\gamma$  cannot be reached.

We display on Fig. 6 (respectively 7) the influence of the pump above threshold  $P$  (respectively the carrier lifetime  $T$ ) and the feedback strength  $\gamma$  on the chaos bandwidth and of the frequency of the ECMs. Increasing  $P$  has the same effect as increasing  $1/T$  (and reversely). The relaxation oscillation frequency is proportional to

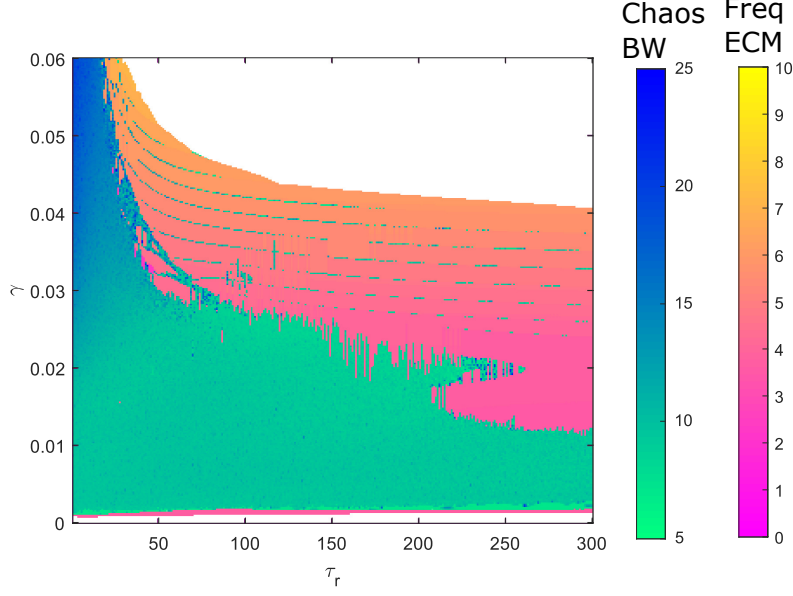


Figure 4. Influence of the finite penetration depth  $\tau_r$  (horizontal axis) and of the feedback strength  $\gamma$  (vertical axis) on the frequency of the external cavity modes for the self-pulsing states (pink to yellow color-scales) and on the chaos bandwidth (green to blue color-scales). The steady-states are displayed in white.

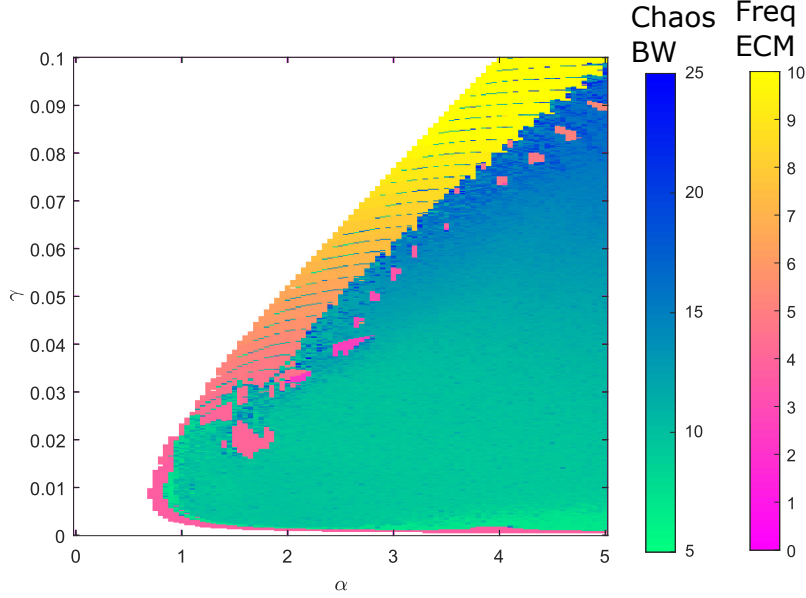


Figure 5. Influence of the  $\alpha$ -factor (horizontal axis) and of the feedback strength  $\gamma$  (vertical axis) on the frequency of the external cavity modes for the self-pulsing states (pink to yellow color-scales) and on the chaos bandwidth (green to blue color-scales). The steady-states are displayed in white.

$\sqrt{P/T}$ <sup>24</sup> and a similar square-root dependency seems to occur for the restabilization value. A strong decrease of  $T$  (i.e.  $T \approx 1$ ) not only enables the apparition of broadband chaos and high-frequency ECMs but also increases the range of low feedback values where the laser remains stable. This condition is often achieved in quantum cascade lasers and this latter result has been confirmed with a more accurate 3-levels model of a QCL subjected to phase-conjugate feedback.<sup>25</sup>

In all these parametric studies, we also observe a direct link between the presence of high-frequency ECMs

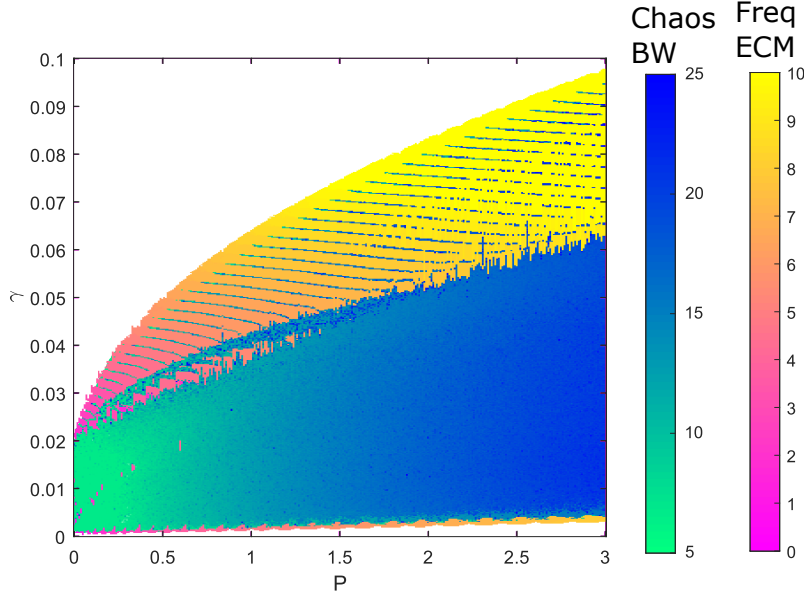


Figure 6. Influence of the pump parameter  $P$  (horizontal axis) and of the feedback strength  $\gamma$  (vertical axis) on the frequency of the external cavity modes for the self-pulsing states (pink to yellow color-scales) and on the chaos bandwidth (green to blue color-scales). The steady-states are displayed in white.

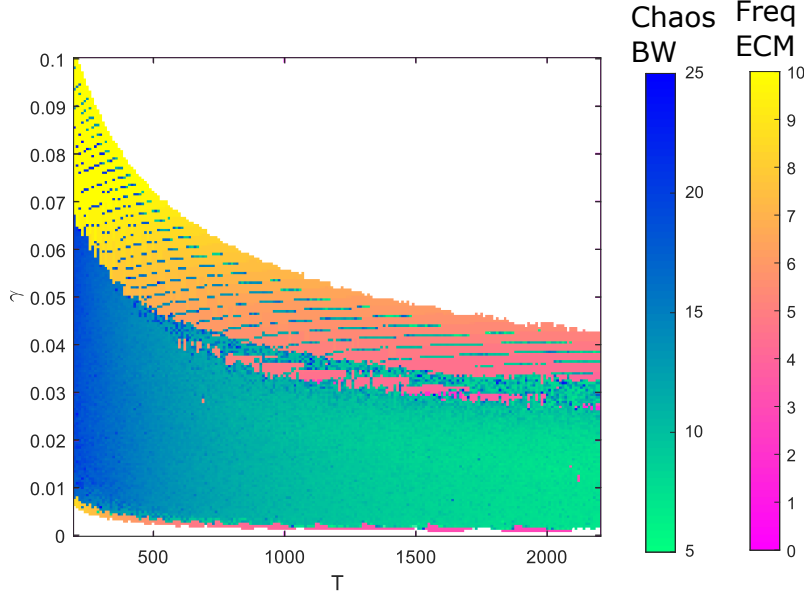


Figure 7. Influence of the carrier lifetime  $T$  (horizontal axis) and of the feedback strength  $\gamma$  (vertical axis) on the frequency of the external cavity modes for the self-pulsing states (pink to yellow color-scales) and on the chaos bandwidth (green to blue color-scales). The steady-states are displayed in white.

and broadband chaos. Both chaos bandwidth and ECM frequency are related to a general "speed" of the system. Furthermore, high values of chaos bandwidth are obtained between two successive ECMs. This result has been also observed experimentally, with a strong enhancement of the chaos bandwidth in the region of the ECMs.<sup>10</sup>

Finally, we study the effective chaos bandwidth. For the default parameters indicated Tab. 1, we plot on Fig. 8 (a) the steady-states, the frequency of the external cavity modes and, for the chaotic states, their effective (chaos) bandwidth and their chaos bandwidth, versus the feedback strength  $\gamma$ . As in a bifurcation diagram, each

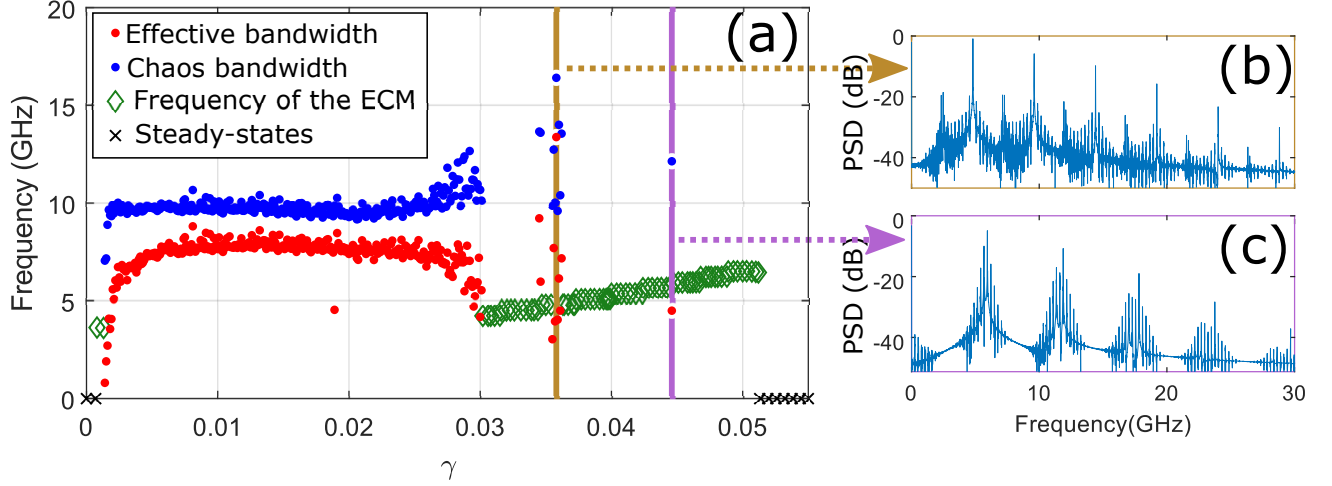


Figure 8. (a) Evolution of chaos bandwidth and effective (chaos) bandwidth (for chaotic states) and oscillation frequency (for ECMs) for a typical laser with phase-conjugate feedback. (b) and (c) present the power spectral density (PSD) for  $\gamma = 0.0358$  (brown line on (a)) and  $\gamma = 0.0446$  (violet line on (a)).

simulation is initialized with the output of the simulation for the previous value of  $\gamma$ . The chaos bandwidth and the effective bandwidth follow the same trend. Moreover, as previously reported the chaos bandwidth rises as the ECMs appears (for  $\gamma > 0.03$ ). At  $\gamma = 0.0358$  (brown vertical bar), the chaos bandwidth equals 16.42 GHz and the effective chaos bandwidth 13.39 GHz. A study of the spectrum of this time series, displayed Fig. 8 (b), shows many frequency components, with a maxima at 4.8 GHz and  $\approx 2.4$  GHz. 4.8 GHz is the frequency of the nearest ECM, while the other is half this value. However, in this region of mixed chaos and ECMs, the effective chaos bandwidth can decrease to low values while the chaos bandwidth remains high. For instance, at  $\gamma = 0.0446$  (violet vertical bar), the effective chaos bandwidth is equal to 4.5 GHz while the chaos bandwidth is as high as 12.15 GHz. A look at the spectrum, see Fig. 8 (c), shows the energy is centered around 5.91 GHz, which is also the frequency of the nearest ECM. This high value of frequency (and the harmonics of this value) enhance the chaos bandwidth but not the effective chaos bandwidth since most of the energy is located on a few values. Fortunately, experimental fluctuations seem to prevent this semi-destabilized ECM to be obtained in reality.<sup>12</sup>

In conclusion, we have studied all the parameters to manipulate the chaos bandwidth and the ECM frequency of a laser diode with phase-conjugate feedback. Both chaos bandwidth and ECM frequency can be enhanced by changing laser properties (pump  $P$ , carrier lifetime  $T$ ,  $\alpha$ -factor) or mirror size (finite penetration depth  $\tau_r$ ). On the other hand, the length of the external cavity has no influence on the chaos bandwidth. This means that once the two phase-conjugate feedback components have been fixed, the chaos bandwidth keeps its value at a given feedback strength  $\gamma$ . Phase-conjugate feedback can therefore be a strong candidate to obtain a robust and broadband chaotic laser source with a semiconductor laser and only one passive component.

## ACKNOWLEDGMENTS

The Chaire Photonique is funded by Ministère de l'Enseignement supérieur, de la Recherche et de l'Innovation, Région Grand-Est, Département Moselle, European Regional Development Fund (ERDF), Metz Métropole, Airbus GDI Simulation; CentraleSupélec and Fondation CentraleSupélec.

## REFERENCES

- [1] Konnerth, K. and Lanza, C., "Delay between current pulse and light emission of a gallium arsenide injection laser," *Applied Physics Letters* **4**, 120–121 (apr 1964).
- [2] Broom, R., "Self modulation at gigahertz frequencies of a diode laser coupled to an external cavity," *Electronics Letters* **5**(23), 571 (1969).



- [3] Heil, T., Fischer, I., Elsässer, W., Krauskopf, B., Green, K., and Gavrielides, A., “Delay dynamics of semiconductor lasers with short external cavities: Bifurcation scenarios and mechanisms,” *Physical Review E* **67**, 066214 (jun 2003).
- [4] Gray, G. R., Huang, D., and Agrawal, G. P., “Chaotic dynamics of semiconductor lasers with phase-conjugate feedback,” *Physical Review A* **49**, 2096–2105 (mar 1994).
- [5] Lawrence, J. S. and Kane, D. M., “Contrasting conventional optical and phase-conjugate feedback in laser diodes,” *Physical Review A - Atomic, Molecular, and Optical Physics* **63**(3), 1–10 (2001).
- [6] Karsaklian Dal Bosco, A., Wolfersberger, D., and Sciamanna, M., “Super-harmonic self-pulsations from a time-delayed phase-conjugate optical system,” *Applied Physics Letters* **105**, 081101 (aug 2014).
- [7] Mercier, É., Weicker, L., Wolfersberger, D., Kane, D. M., and Sciamanna, M., “High-order external cavity modes and restabilization of a laser diode subject to a phase-conjugate feedback,” *Optics Letters* **42**, 306 (jan 2017).
- [8] Sciamanna, M. and Shore, K. A., “Physics and applications of laser diode chaos,” *Nature Photonics* **9**, 151–162 (mar 2015).
- [9] Mercier, É., Wolfersberger, D., and Sciamanna, M., “High-frequency chaotic dynamics enabled by optical phase-conjugation,” *Scientific Reports* **6**, 18988 (may 2016).
- [10] Malica, T., Bouchez, G., Wolfersberger, D., and Sciamanna, M., “Spatiotemporal complexity of chaos in a phase-conjugate feedback laser system,” *Optics Letters* **45**, 819 (Feb. 2020).
- [11] Erneux, T., Gavrielides, A., Green, K., and Krauskopf, B., “External cavity modes of semiconductor lasers with phase-conjugate feedback,” *Physical Review E - Statistical Physics, Plasmas, Fluids, and Related Interdisciplinary Topics* **68**(6) (2003).
- [12] Bouchez, G., Uy, C.-H., Macias, B., Wolfersberger, D., and Sciamanna, M., “Wideband chaos from a laser diode with phase-conjugate feedback,” *Optics Letters* **44**, 975 (feb 2019).
- [13] He, G. S., “Optical phase conjugation: principles, techniques, and applications,” *Progress in Quantum Electronics* **26**, 131–191 (may 2002).
- [14] Feinberg, J., “Self-pumped, continuous-wave phase conjugator using internal reflection,” *Optics Letters* **7**, 486 (oct 1982).
- [15] Lang, R. and Kobayashi, K., “External optical feedback effects on semiconductor injection laser properties,” *IEEE Journal of Quantum Electronics* **16**, 347–355 (mar 1980).
- [16] Agrawal, G. P. and Klaus, J. T., “Effect of phase-conjugate feedback on semiconductor laser dynamics,” *Optics Letters* **16**, 1325 (sep 1991).
- [17] Murakami, A. and Ohtsubo, J., “Dynamics and linear stability analysis in semiconductor lasers with phase-conjugate feedback,” *IEEE Journal of Quantum Electronics* **34**(10), 1979–1986 (1998).
- [18] DeTienne, D., Gray, G., Agrawal, G., and Lenstra, D., “Semiconductor laser dynamics for feedback from a finite-penetration-depth phase-conjugate mirror,” *IEEE Journal of Quantum Electronics* **33**, 838–844 (may 1997).
- [19] Weicker, L., Erneux, T., Wolfersberger, D., and Sciamanna, M., “Laser diode nonlinear dynamics from a filtered phase-conjugate optical feedback,” *Physical Review E* **92**, 022906 (aug 2015).
- [20] Weicker, L., Uy, C.-H., Wolfersberger, D., and Sciamanna, M., “Mapping of external cavity modes for a laser diode subject to phase-conjugate feedback,” *Chaos: An Interdisciplinary Journal of Nonlinear Science* **27**(11), 114314 (2017).
- [21] Lin, F. Y. and Liu, J. M., “Chaotic lidar,” *IEEE Journal on Selected Topics in Quantum Electronics* **10**(5), 991–997 (2004).
- [22] Lin, F. Y., Chao, Y. K., and Wu, T. C., “Effective Bandwidths of Broadband Chaotic Signals,” *IEEE Journal of Quantum Electronics* **48**, 1010–1014 (aug 2012).
- [23] Mercier, É., Uy, C.-H., Weicker, L., Virte, M., Wolfersberger, D., and Sciamanna, M., “Self-determining high-frequency oscillation from an external-cavity laser diode,” *Physical Review A* **94**, 061803 (dec 2016).
- [24] Friart, G., Weicker, L., Danckaert, J., and Erneux, T., “Relaxation and square-wave oscillations in a semiconductor laser with polarization rotated optical feedback,” *Optics Express* **22**, 6905 (Mar. 2014).
- [25] Weicker, L., Wolfersberger, D., and Sciamanna, M., “Stability analysis of a quantum cascade laser subject to phase-conjugate feedback,” *Physical Review E* **98**, 012214 (jul 2018).